SCI. MAR., 64 (4): 393-402 SCIENTIA MARINA 2000

Side scan sonar image and geologic interpretation of the Ría de Pontevedra seafloor (Galicia, NW Spain)*

SOLEDAD GARCÍA-GIL, RUTH DURÁN and FEDERICO VILAS

Departamento de Geociencias Marinas y Ordenación del Territorio, Facultad de Ciencias, Universidad de Vigo, Apdo. 36200, Vigo, Spain. E-mail: sgil@uvigo.es, r.duran@uvigo.es, fvilas@uvigo.es.

SUMMARY: High-resolution side scan sonar has been used for mapping the seafloor of the Ría de Pontevedra. Four backscatter patterns have been mapped within the Ría: (1) Pattern with isolated reflections, correlated with granite and metamorphic outcrops and located close to the coastal prominence and Ons and Onza Islands. (2) Pattern of strong reflectivity usually located around the basement outcrops and near the coastline and produced by coarse-grained sediment. (3) Pattern of weak backscatter is correlated with fine sand to mud and comprising large areas in the central and deep part of the Ría, where the bottom currents are weak. It is generally featureless, except where pockmarks and anthropogenic features are present. (4) Patches of strong and weak backscatter are located in the boundary between coarse and fine-grained sediments and they are due to the effect of strong bottom currents. The presence of megaripples associated to both patterns of strong reflectivity and sedimentary patches indicate bedload transport of sediment during high energy conditions (storms). Side scan sonar records and supplementary bathymetry, bottom samples and hydrodynamic data reveal that the distribution of seafloor sediment is strongly related to oceanographic processes and the particular morphology and topography of the Ría.

Key words: seafloor texture, high resolution seafloor mapping, side scan sonar, bedforms, Ría de Pontevedra, rías, Galicia.

INTRODUCTION AND PREVIOUS WORK

The first detailed maps of the Ría de Pontevedra deal with textural distribution of seafloor sediments in terms of grain-sized ternary diagrams, carbonated and organic matter contents, based on regularly spaced bottom samples (Vilas *et al.,* 1996). Other papers on this Ría are related with the study of the content and distribution of heavy metals in the sediments (Rubio *et al.,* 1995, 1996).

More recently, the published papers on the Ría de Pontevedra are concerned with the origin and sedimentary infill of the Ría (García-Gil *et al.,* 1999) based on the high resolution seismic interpretation.

*Received February 24, 2000. Accepted May 9, 2000.

High resolution seafloor mapping techniques such as side scan sonar have been shown to be very useful tools for recognising sedimentary environments (Knebel, 1995, 1996, 1999), geological mapping (Schwab, in press) and also for the study of sedimentary bedforms (Leckie, 1988; Hequette, 1995; Schwab, 1996; Okyar, 1997).

The main target of this paper is to undertake detailed mapping of the seafloor of Ría de Pontevedra using side scan sonar records. This high-resolution technique gives a continuous record of the present seafloor allowing the accurate distribution of outcrops, sediment, anthropogenic features and bedforms. It is not possible to provide such comprehensive coverage using a sampling grid.

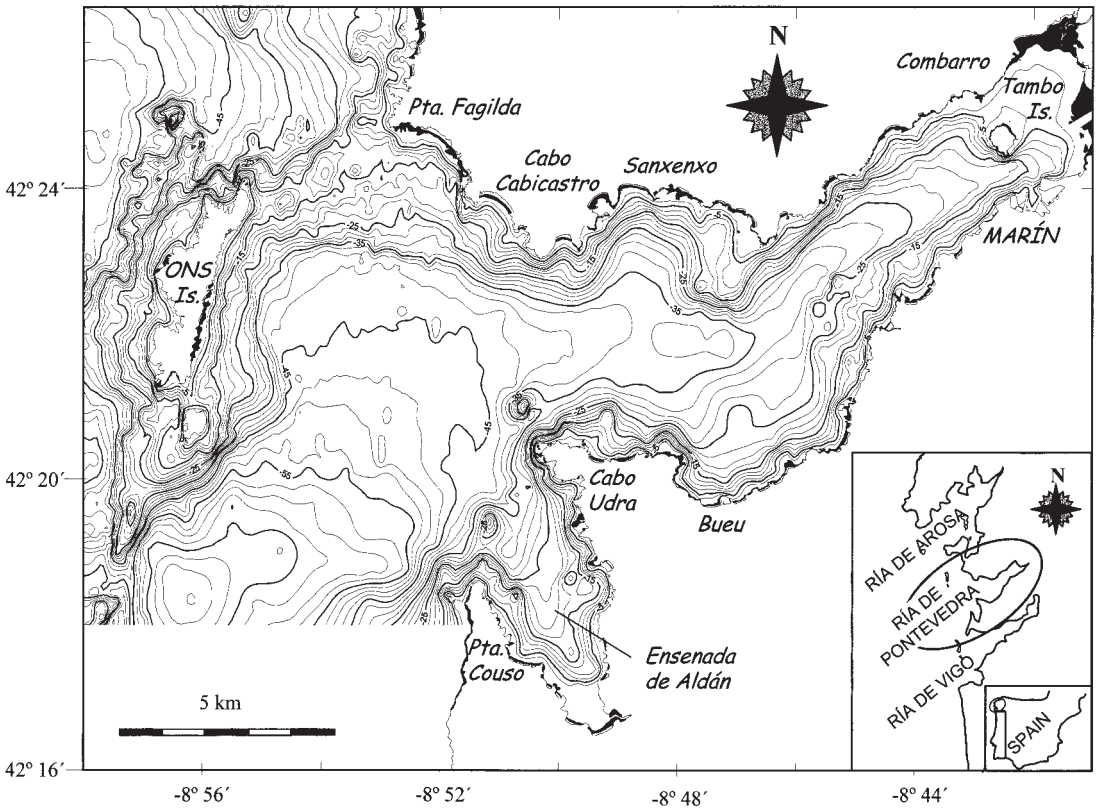

FIG. 1. – Bathymetric map (in metres) of the Ría de Pontevedra. Insert maps show locations of the Rías in Northwest Spain and the Ría de Pontevedra study area.

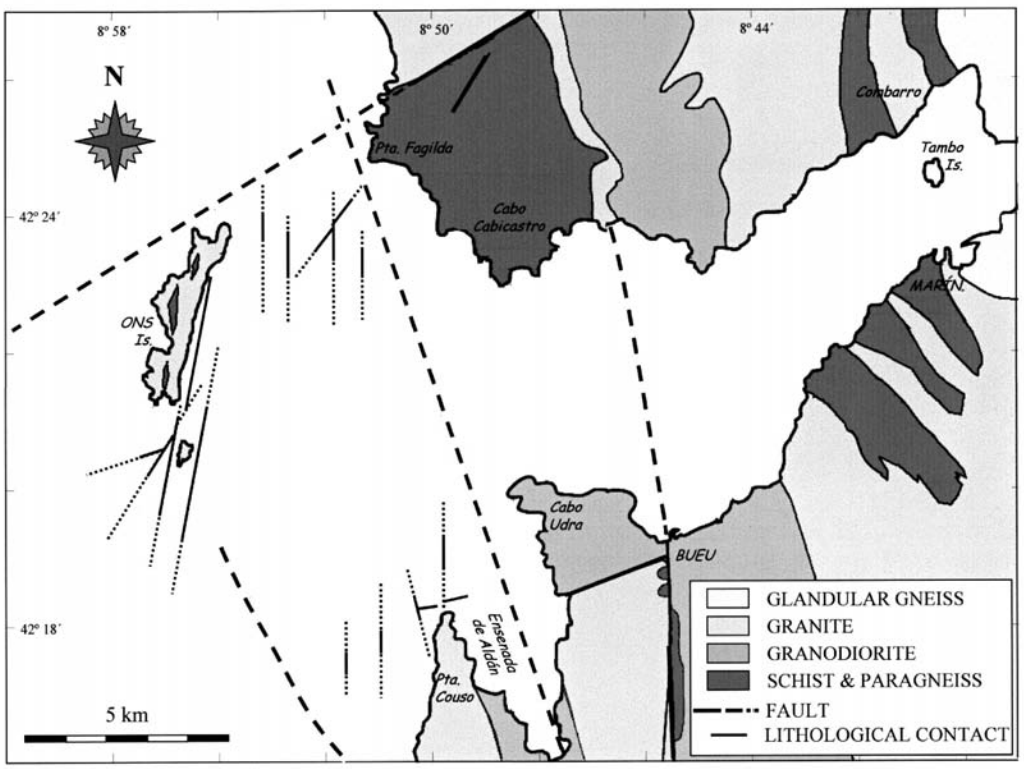

FIG. 2. – Modified geotectonic map of the Ría de Pontevedra. Solid lines represent land faults from the geological map (IGME 1987). Gross dashed lines are the interpreted faults from seismic Uniboom records (García-Gil *et al.*, 1999). Thin dashed lines are the faults interpreted from the SSS images in this paper.

SETTING

Von Richtofen (1886) defined the term Ría as a funnel-shaped drowned valley on coasts that are transverse to the Palaeozoic trends.

The Ría de Pontevedra is the third in size of the Rías (64.5 km^2), after the Ría de Arosa and Vigo (Fig. 1). The Ría shows a funnel-shaped in plan view having a N45E orientation, except in the Ensenada de Aldán, which has a NNW trend. The major axis of the Ría has a maximum length of 28 km. The maximum width (12 km) occurs between Punta Fagilda and Cabo Osas Cape, and decreases from this point towards the inner part of the Ría.

The bathymetry of the Ría shows valley geometry, with the deepest part located along the central axes. At the north of the islands, between Ons and Fagilda Cape, the topography is characterised by shallow depths (less than 15 m), although at the south the depth reaches more than 50 m.

Along its NE-SW axes the depth decreases gradually from outer to inner parts. Topography disrupted mainly at the outer areas of the Ría by faults controlled basement high (García-Gil *et al*, 1999).

According to the geological map (Fig. 2), the country rock in the Ría de Pontevedra consists mainly of post Hercynian orogenic plutonic and Paleozoic metamorphic rocks with a N-S and NNE-SSW structural trend.

Recently García *et al*. (1999) provided additional data on the tectonic-eustatic processes which controlled the evolution of Ría de Pontevedra. The entrance of the Ría is partially blocked by a North trending ridge whose crests are Ons and Onza Islands separated by a narrow and shallow channel. The Ría de Pontevedra and the Islands at its mouth have rectilinear trends indicating that they are tectonically controlled. The Northeast side of the Ría also shows a rectilinear trending northeast-southwest, which suggests that this side also may be fault controlled and that a fault extends southwestward along the northeast side of the Ría from its mouth up to Ons and Onza Island ridge.

HYDRODYNAMICS

Water circulation in the Ría shows a dominant anticlockwise pattern. The current-meter data (ENCE, 1979; MOPU, 1980) show a coincidence between the near-bottom current and the tidal currents (Fig. 3). The marine water influx dominated all the measurements made during the flood and it is important during the ebb along the south coast. On the north coast the current-meter data reveal a net outflow. In both sides of the Ría, Bueu and Sanxenxo bays the distribution of the near-bottom currents are significantly different, showing the presence of eddies near the coast (Ruiz Mateo, 1983).

This circulation pattern appears to be controlled by the topography (Fig. 1), which provokes eddies on the north and south coast (Ruiz Mateo, 1983). Current-meter data show a weak mean tidal velocity (4-6 cm/s), although the velocities are locally variable due to the irregular basin topography. It is noted that the magnitude of the flow is significantly reduced in the inner part of the Ría (Fig. 3). Maximum near-bottom tidal currents generally do not exceed 14 cm/s within the Ría basin (ENCE, 1979; MOPU, 1980), but this rises to 44 cm/s at the north entrance of the Ría (B. Martín and L. Fariña, pers. com).

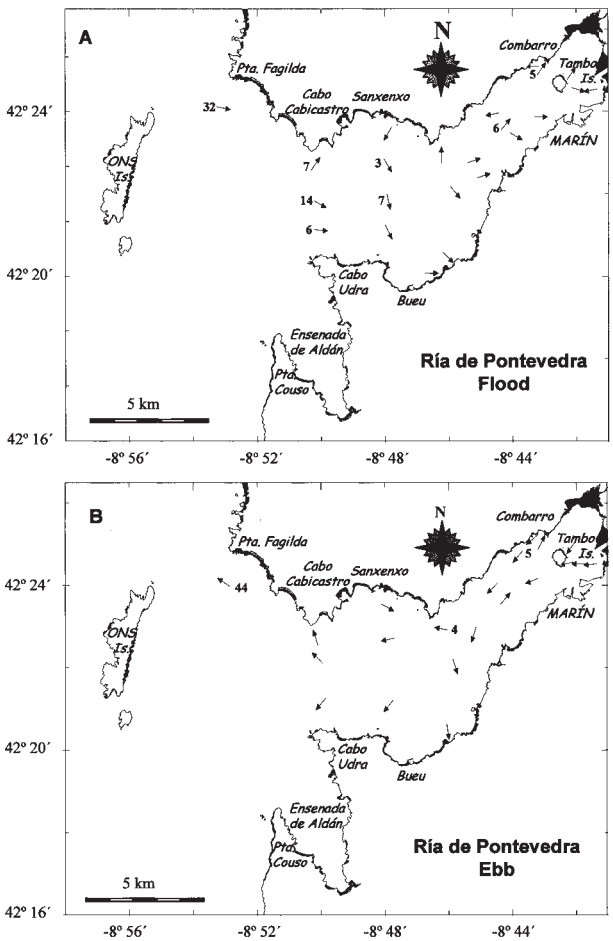

FIG. 3. – Location of the current-meter stations. Arrows indicate the tidal current directions and the numbers give the current velocity in cm/s for flood (A) and ebb conditions (B). Data from ENCE (1979), MOPT (1980) and B. Martín and L. Fariña. (pers. com.)

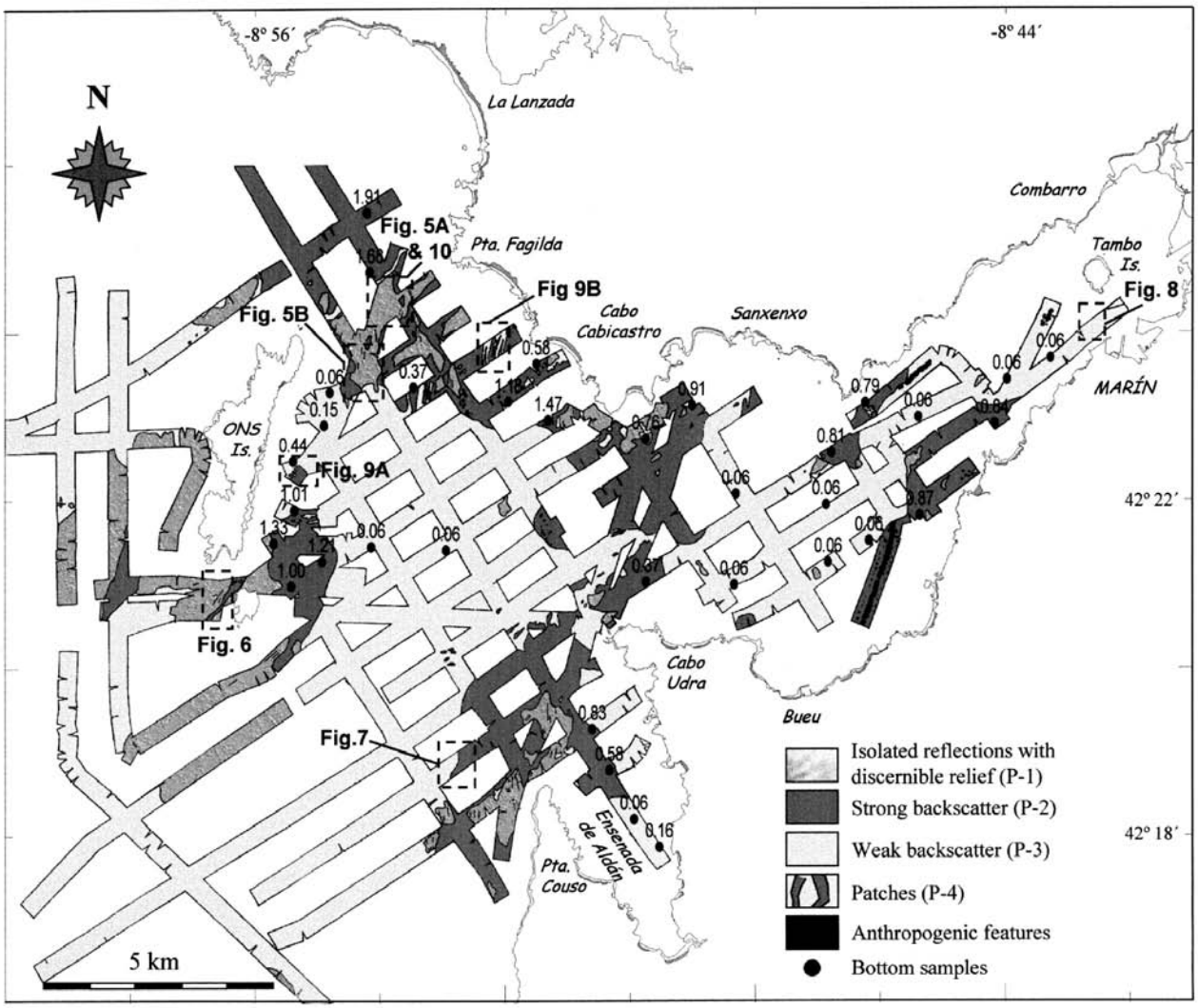

FIG. 4. – Sea-floor mapping of backscatter patterns based on side scan sonar image. Numbers correspond to the grain size of bottom samples (in millimeters). Boxes show location of the figures.

In the inner part of the Ría, the water currents are usually weaker. A net outflow at the southeast of Tambo Island measured by the current-meter is probably due to outflow of the Lérez River and the local bathymetry (Ruiz Mateo, 1983).

The weather conditions play an important role in the formation of waves and currents that control the sedimentation processes in the Ría (Vilas *et al.*, 1996). The main winds in the Ría have a frequent direction parallel to the axis of the Ría (NE-SW), with an average velocity of 10 to 30 km/h. Circulation system in the Ría de Pontevedra can be affected by storms, which induce oscillatory and wave drift currents from the southwest during winter (mainly from December to February) and from northwest during the summer. It is noticeable that intense wave agitation affecting the shelf bottom accompanies these storm-surges.

SURVEY

The side scan sonographs of the seafloor were collected along 320 Km of tracklines within the study area in July 1996, onboard the vessel V. Paz Andrade. These geophysical data were acquired using a Klein 595 side scan sonar, that operated at a frequency of 500 kHz and scanned 200 m to each side of the ship's track. Simultaneously, seismic reflection profiles were obtained with a 300 joule EG&G Geopulse. The survey lines were performed following a predetermined grid which covers the whole Ría (Fig. 4). Positioning was achieved by using a differential GPS.

The side scan towfish was navigated relative to the ship. The position of the towfish was calculated assuming that it was directly behind the research vessel; i.e., that it followed the ship trackline. This

assumption is relatively accurate when the research vessel is running in a straight line, with a small amount of tow cable deployed. The system has an automatic speed correction and the side scan sonar data were processed geometrically.

BACKSCATTER PATTERNS

The backscatter pattern and facies distributions have been interpreted using different supplemental marine geological and sedimentological data. Which include: (1) high-resolution seismic profiles (Uniboom); (2) geological map; (3) bottom samples at fixed stations (Fig. 4); (4) bottom sediment distribution maps (Vilas *et al*., 1996); and (5) the detailed bathymetry of the Ría produced in this study (Fig. 1).

Different types of seafloor materials produce distinct return on side scan sonar records, based on their degree of reflectivity, amount of surface relief and others features. In the sonographs, lighter tones indicated areas which produce weak backscatter, such as mud and sand (Belderson, 1972); whereas

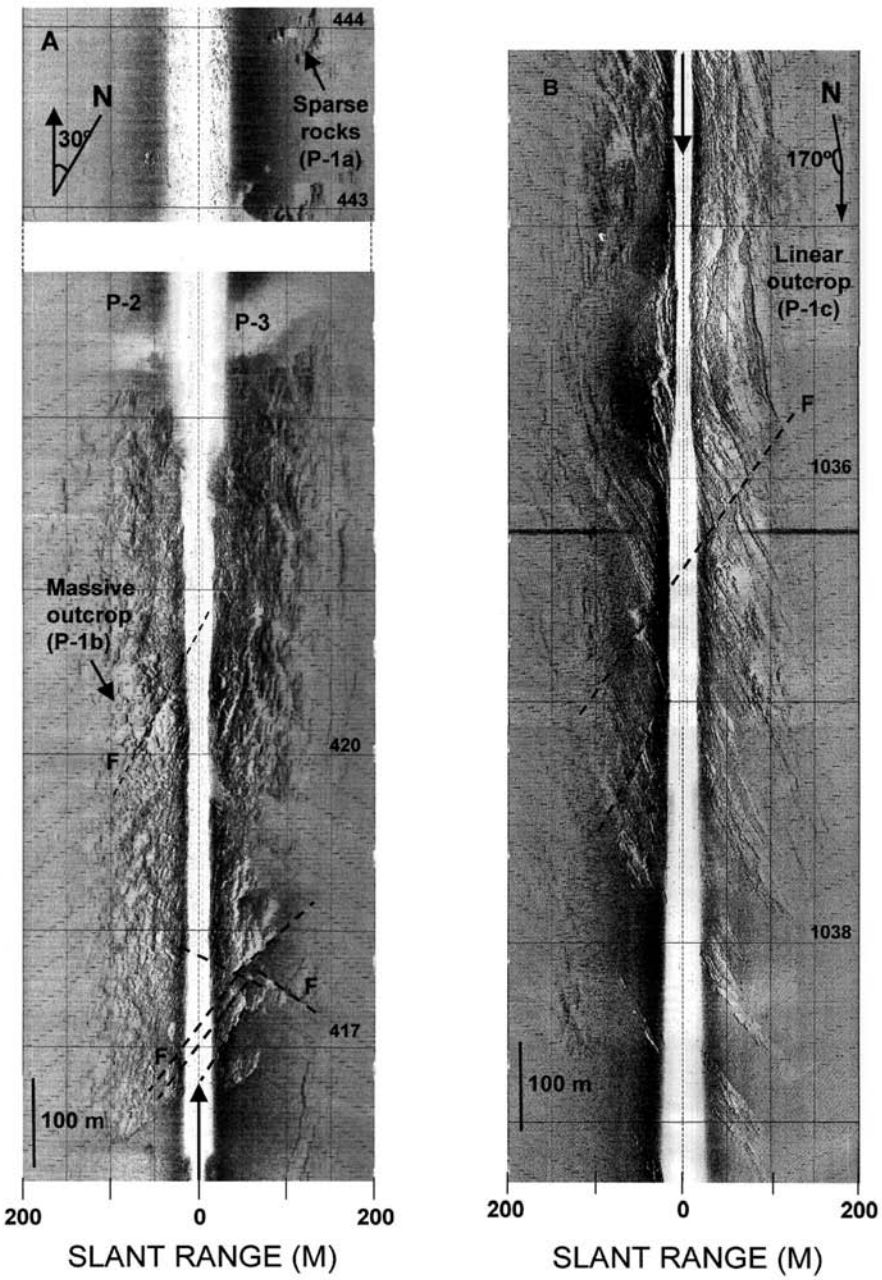

FIG. 5. – Sonograph showing the characteristic feature of Pattern-1. (A) Speckled (P-1a) and Blotchy (P-1b) appearance interpreted as basement granite outcrops. (B) Linear outcrop (P-1c) showing a faulted (F) metamorphic basement. Shadows appear white. See Fig. 4 for location.

darker tones depicted strong acoustic reflectivity, shells, gravel and coarse-grained sand will send back much more of the incident sound (Belderson, 1972). Where the acoustic contact is too weak between coarse and fine sediments, this contact has been determinated taking into account the characteristic of the direct bottom samples located on the sonographs.

In the Ría de Pontevedra four different acoustic patterns were recognised: (1) Pattern with isolated reflections, (2) pattern of strong backscatter, (3) pattern of weak backscatter, and (4) patches of strong and weak backscatter (Fig. 4).

Pattern 1 (P-1), with isolated reflections and high relief (Fig. 5). This pattern has been interpreted in other shelves as produced by outcrops (Belderson, 1972, Knebel, 1995, Barnhardt, 1998). In the Ría de Pontevedra, this pattern is characterised by a strong surface return (dark grey to black on the sonographs) and high bathymetric relief and fractures resulting in areas with acoustic shadows (Fig. 5). This pattern includes three different appearances:

(a) Speckled (P-1a), small and rounded features (Fig. 5A) interpreted as sparse rocks according to Knebel (1995).

(b) Blotchy (P-1b), large features with discernible relief and frequently affected by tectonic fractures (Fig. 5A and 6), interpreted by other authors as massive rocks according to Belderson (1972), Knebel (1995) and Barnhardt (1998).

(c) Linear (P-1c), high reflectivity and discernible relief but less prominent than in the blotchy pattern. The presence of folding structures as well as faults is also characteristic from this pattern P-1c (Fig. 5B).

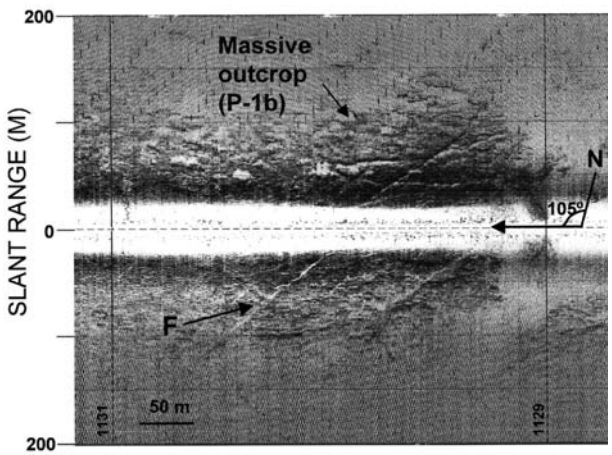

FIG. 6. – Detail of faults (F) NE-SW orientated affecting a blotchy granite outcrop (P-1b). Shadows in white. See Fig. 4 for location.

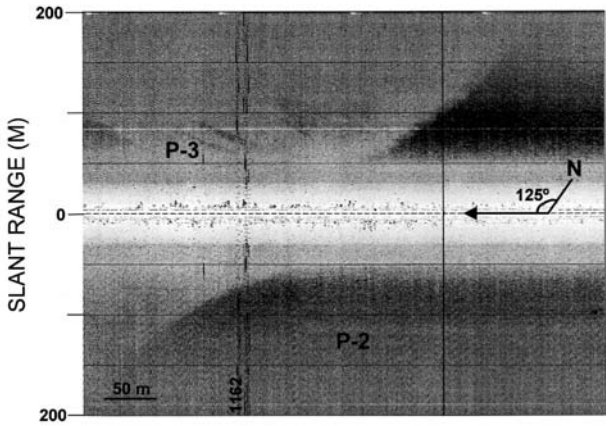

FIG. 7. – Sonograph showing a sharp boundary between both, pattern of strong backscatter (P-2) in dark grey (coarse sand to gravel) and pattern of weak backscatter (P-3) in light grey (fine grained sand and mud). See Fig. 4 for location.

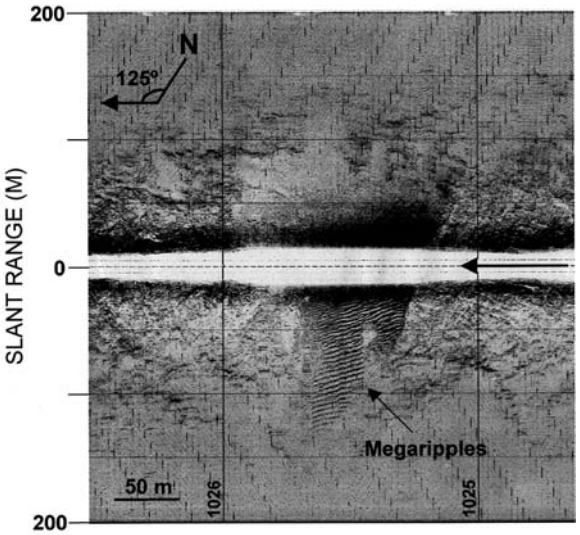

FIG. 8. – Sonograph showing a train of straight bifurcated megaripples crests with a wavelength of 3.33 m developed on coarse grained sediments, and located between granite outcrops at the north entrance of the Ría. See Fig.4 for location.

Pattern 2 (P-2), relative strong backscatter (dark grey to black on the sonographs), that appear as nearly uniform dark sonographs (Fig. 7). The bottom samples (Fig. 4) shows that this pattern corresponds to sandy gravel and coarse to medium sand. The local presence of bedforms as megaripples associated to this pattern is characteristic (Fig. 8).

Pattern 3 (P-3), weak backscatter (light grey to white on the sonographs) and generally featureless (Fig. 7). The bottom samples (Fig. 4) corresponding to the areas with this pattern are composed of fine sand and mud. The presence of pockmarks is noticeable (Fig. 9) associated to this pattern.

Pattern 4 (P-4), high and low reflectivity patches. Two types were distinguished: P-4a, irregular

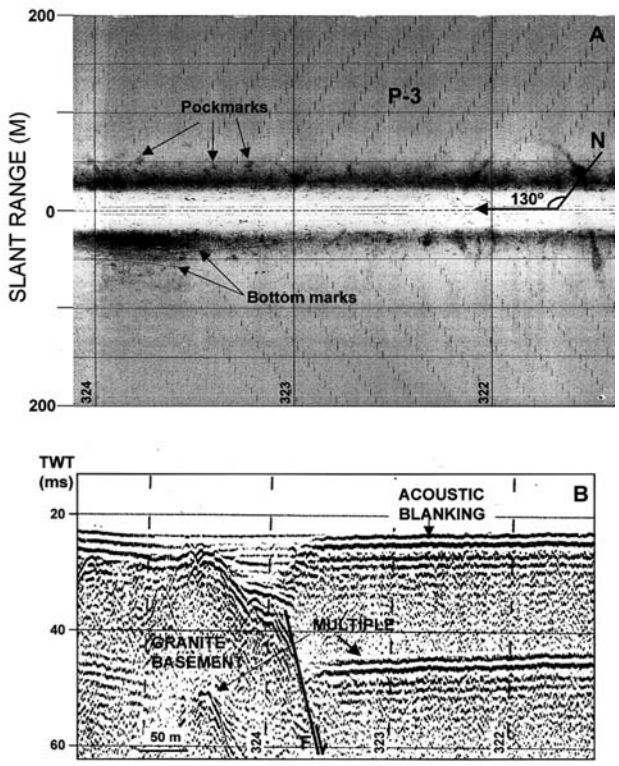

FIG. 9. – (A) Sonograph showing the pattern of weak backscatter (Pattern 3) with circular to elliptical high reflectivity spots interpreted as pockmarks. Anthropogenic features also appear. (B) Uniboom seismic record with a very shallow acoustic blanking due to the presence of gas in sediments. See Fig. 4 for location.

shaped patches with a strong backscatter, usually on the weak reflectivity area and viceversa (Fig. 10A); P-4b, longitudinal patches, that usually are located on the transition zone from fine to coarse grained sediment (Figs. 4 and 10B).

RESULTS AND DISCUSSION

From the interpretation of the sonograph mosaic from the Ría de Pontevedra seafloor a spatial distribution of the four different patterns described above can be recognised.

Pattern 1a (speckled) appears widespread through the whole study area showing low morphological relief and reduced surface. P-1a represents scarce outcrops of basement rocks (Fig. 4).

Pattern 1b (blotchy) is located in the outer part of the Ría (Figs. 4 and 11) around the Ons and Onza Islands, as well as close to the coastal prominence of the Ría (Pta. Couso, Pta. Fagilda and Cabo Cabicastro). P-1b extends over larger areas and has higher relief than P-1a. Comparing the location of P-1a and P-1b with the geological map (Fig. 2) their coincidence in the spatial continuity within the granitic domains can be observed, thus these patterns (P-1a and P-1b) may be interpreted as granitic outcrops.

Pattern 1c (linear) occurs only at the north entrance to the Ría (Figs. 4 and 11). This sector (Fig. 2) coincides with both the boundary location between granites and metamorphic rocks and the presence of several major faults, which are clearly shown on the sonar images (Fig. 5b). Therefore, this pattern (P-1c) has been interpreted as corresponding to metasediment outcrops controlled by faults.

The coincidence between the orientation of the faults affecting both granite and metamorphic outcrops and the main faults distinguished on land (NE-SW, NNW-SSE and N-S) (Fig. 2) is important.

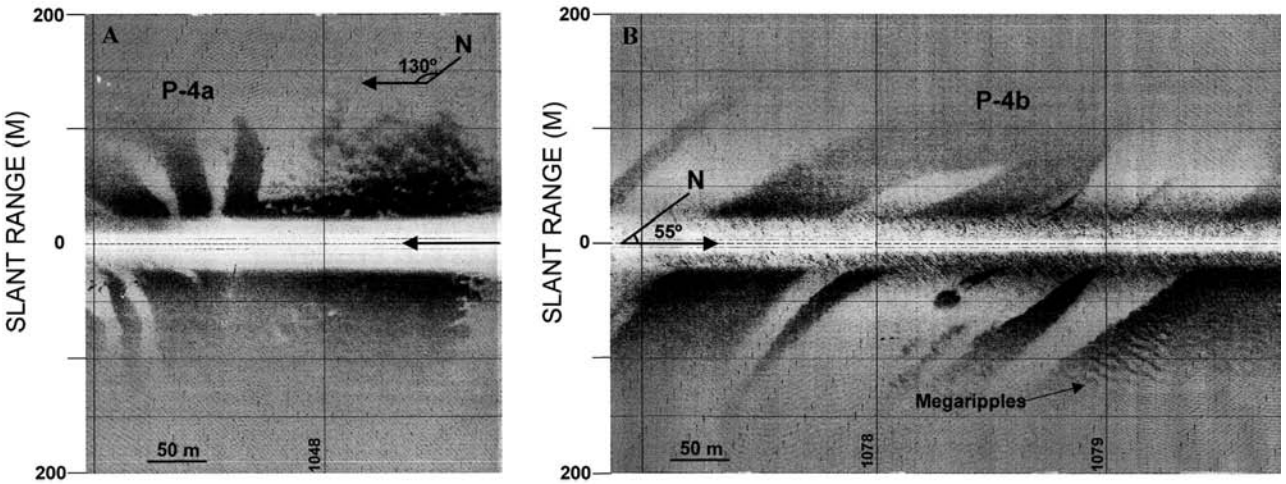

FIG. 10. – Sonograph showing irregular tonal patches produced by textural difference in the sediments. Dark grey patches represent coarse-grained sediment onto fine sand (light grey). (A) Irregular patches and (B) longitudinal patches. Megaripples appear in some patches of strong backscatter. See Fig. 4 for location.

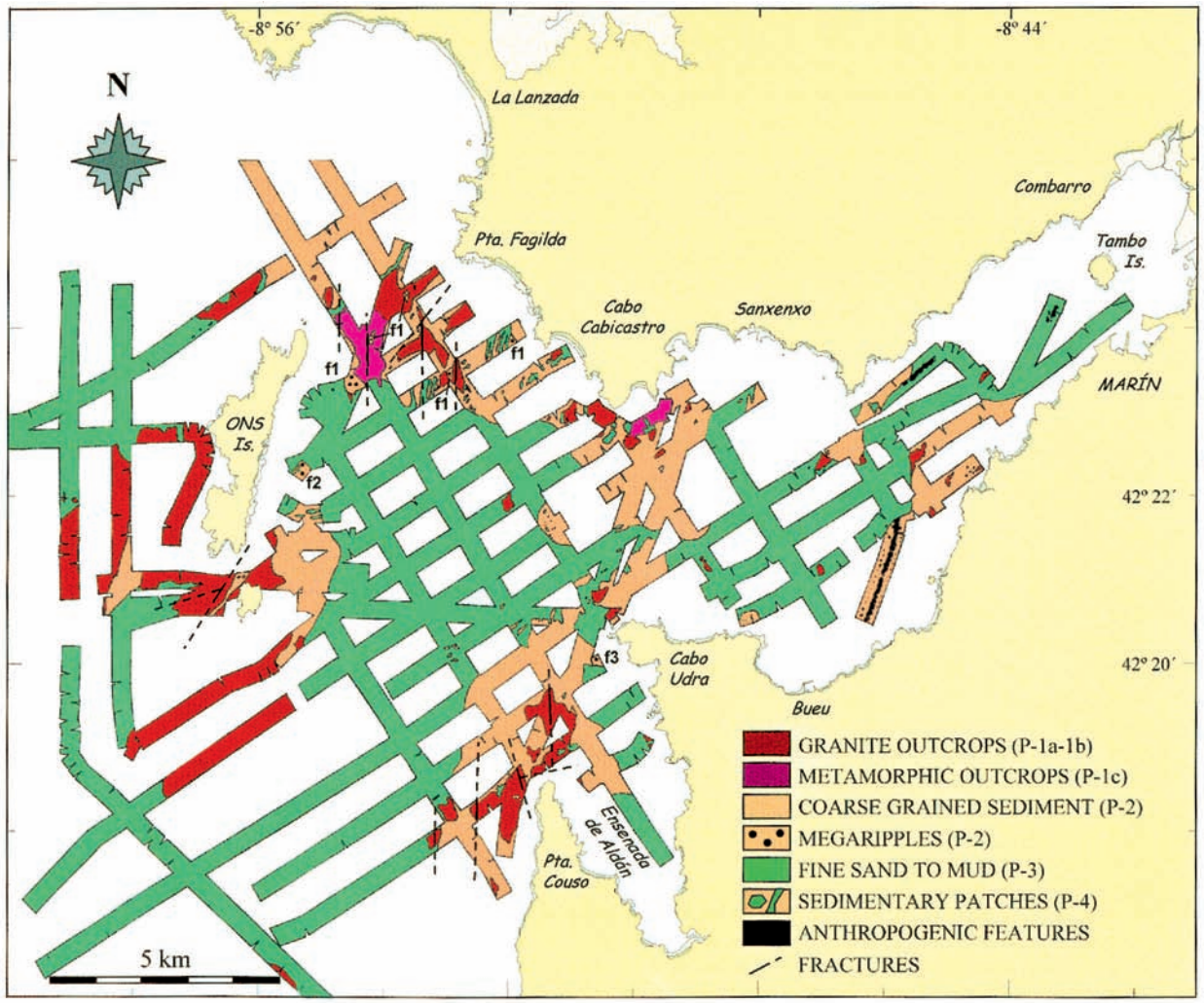

FIG. 11. – Geological sea-floor mapping interpretation based on the backscatter patterns. Megaripples fields are indicated as f1, f2 and f3

The pattern-2 is located preferentially close to the coastline and surrounding the different outcrops represented by pattern-1, as well as in the north-south trending band between Cabo Cabicastro and Cabo Udra (Figs. 4 and 11). Taking into account the bathymetric map the direct relationship between the pattern-2 location and shallower water depth is very clear. In fact, the above-mentioned north-south belt Cabo Cabicastro-Cabo Udra corresponds with a flatter seabed area where the Ría starts to be narrower.

The most characteristic feature of this pattern-2 is the local presence of megaripples. These bedforms into the Ría are composed by coarse sands and gravel and show straight to slightly sinuous bifurcated crests (Fig. 8). The wavelengths measured from the sonograph records range from 0.91 to 7.73 m.

Taking into account all the above mentioned characteristics, P-2 can be interpreted as hydrodynamically controlled.

Three ripples fields have been distinguished within pattern-2 according to its geographical location (Fig. 11) as follows:

Field 1, the shallowest, located at the north entrance to the Ría (Fig. 11). Its wavelength shows the wider range, from 0.91 to 7.73 m, although the most frequent are 1.7-2.08 m. The crests are bifurcate with a NNE-SSE and NE-SW orientation (Fig. 8). In this area the sediments are composed of coarse sands (Fig. 4) and the maximum velocity from near-bottom current-meters are 44 cm/s. These bedforms are thought to be formed by waves during storms in the most external sector of the Ría.

Field 2, is at the back of Ons Island and also occurs in shallow water depth. The megaripple wavelength is 1.38 m with a bifurcated crest orientation of N60ºE, oblique to the shoreline. The grain size corresponds to medium-coarse sands (Figs. 4 and 11). Considering all the available data, these

megaripples are also interpreted as due to bottom currents during storm conditions.

Field-3. Located close to Cabo Udra (Fig. 11) at the south coast of the Ría. Wavelengths range from 1.38 to 2 m and the sediment size corresponds to coarse sands. The orientation of the crests is variable depending on their location in this field. These megaripples are interpreted as due to high-energy conditions, such as storms.

Pattern 3. Located in the central and deep part of the Ría. These zones represent the areas where the bottom current velocities shown by the current-meter data are the lowest (Figs. 3 and 11). According to the bottom samples (fine sand to mud) located on the sonographs (Fig. 4) and the weak tidal bottom currents (less than 14 cm/s), this pattern is interpreted as a sub-environment of low energy conditions which justify the lack of sedimentary features.

Nevertheless, the occurrence of pockmarks and anthropogenic features on the cohesive seafloor represented by this pattern-3 can be observed (Figs. 9 and 11). These pockmarks appear as high reflectivity circular to ovoid shapes on the side scan sonar records (Hovland and Judd, 1988). The circular pockmarks in the Ría have a radius ranging from 1.6 m to 4.8 m. The elliptical pockmarks show a length-to-breath ratio ranging from 1 to 1.5, with 3.2 m to 8 m of maximum axes and 2.4 to 6.9 m of minimum axes.

These pockmarks are located in the inner part of the Ría near to Tambo Island (Fig. 9A), where the Uniboom seismic records (Fig. 9B) reveal the occurrence of shallow gas. The anthropogenic marks present in this area could be a mechanism of gas escape activation (García-García *et al*, 1999).

Pattern 4. The two types of sedimentary patches have a different location within the Ría. Irregular shaped patches with a strong backscatter (P-4a), usually on the weak reflectivity area and viceversa (Fig. 10A and 10B) have a widespread distribution into the Ría. Longitudinal patches (P-4b), are usually located on the transition zone from fine grained to coarse sediment (Rao, 1989), and where the bottom currents are stronger. The orientation of these linear patches has a strong correlation with the direction of the near-bottom current given by the current-meter (Fig. 3 and 11).

Worldwide studies (Belderson, 1972; Knebel, 1995, 1996, 1999; Rao, 1989; Okyar *et al.*, 1997) show that these tonal patches reflect textural changes in the bottom sediment that have been generated by high bottom-currents (Kuijpers *et al.*, 1993; Héquette *et al.*, 1995). These features are produced by a combination of erosion and deposition (Knebel, 1991, 1999a, 1999b). Rao (1989) proposed two theories about the origin: (1) based on the topography, in zones where the bathymetry is irregular, the fine sediments are deposited between the undulations; and (2) is based primarily on the wave induced bottom currents. These patches as well as gravelly sediments and rock outcrops occur in areas of strong bottom currents (Okyar *et al.*, 1997).

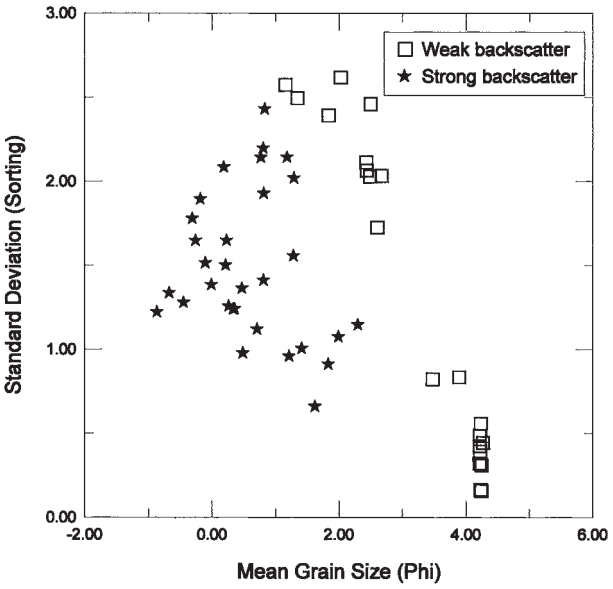

FIG. 12. – Relation between mean grain size (in phi-units) and standard deviation (sorting) of the bottom samples located on the sonographs, taking into account their occurrence within both patterns, high (P-2) and low backscatter (P-3). See text for explanation.

In the study region both high and low backscatter were found associated to the medium grained sands. In order to clarify the reason for this, sedimentological analysis was carried out. The relation between sorting and mean grain size (Fig. 12) reveals that in the medium size sands, the main factor controlling the intensity of backscatter is the sorting, in the sense that high sorting produces low backscatter, increasing as the sorting decreases.

CONCLUSIONS

The interpretation of side scan sonar records together with the bottom samples analysis has provided a much more accurate map of the present seafloor of the Ría de Pontevedra. The use of this high-resolution technique has permitted four sonograph patterns to be distinguished, that have been correlated with the seabed textures. Pattern-1, with

isolated reflections, has been interpreted as produced by different morphologies of granite and metamorphic basement outcrops in this region.

Pattern-2, of strong backscatter, occurs where the sediment texture is coarse-grained (coarse sand to gravel) and shows megaripples in some places. These bedforms can be generated during periods of high-energy conditions on the coast (storms).

On the contrary, pattern-3, weak backscatter, is represented by the areas of finest texture (fine sand to mud), occurring in the Ría areas where the hydrodynamic conditions are enough to permit settling of the sediments. Pockmarks appear on the sonographs of this pattern, being the morphological expression of gas escapes. Anthropogenic features have also been distinguished.

Pattern-4, strong and weak backscatter, is interpreted as sedimentary patches due to strong bottom currents.

The backscatter has been correlated with the sorting of the medium grain sand interval a reverse relationship being found: lowest sorting relating to highest backscatter.

ACKNOWLEDGEMENTS

We would like to thank our colleagues Dr. A. Judd (University of Sunderland) who read the last version of the manuscript and J. Acosta and P. Herranz (Instituto Español de Oceanografía) for their help and comments to elaborate the preliminary steps of the mosaic of side scan sonar. We also thank the project "Dinámica y variabilidad termohalina de las rías gallegas" for providing data on dynamics of waters in the Ría de Pontevedra. This paper is a contribution to the CICYT Projects MAR95-1953 and MAR97-0626.

REFERENCES

Barnhardt, W.A., J.T. Kelley, S.M. Dickson and D.F. Belknap. – 1998. Mapping the Gulf of Maine with side scan sonar: a new bottom-type classification for complex seafloors. *J.Coast. Res.*, 14 (2): 646-659.

Belderson, R.H., N.H. Kenyon, A.H. Stride and A.R Stubbs. – 1972. *Sonographs of the Sea Floor: A picture Atlas*. Elsevier Scientific Publ. Co., Amsterdam.

ENCE. – 1979. *Estudio oceanográfico de la Ría de Pontevedra*. Informe Técnico. Inst. Esp. Oceanogr. Dpto de Oceanografía Física: 1-258.

García-García, A., F. Vilas-Martín and S. García-Gil. – 1999. A seeping sea-floor in a Ría environment: Ría de Vigo (NW Spain). *Environ. Geol.*, 38(4): 296-300.

García-Gil, S., A. García-García and F. Vilas-Martín. – 1999. Identificación sísmico- acústica de las diferentes formas de gas en la Ría de Vigo (NO España). *Rev. Soc. Geol. España*, 12(2): 301-307.

García-Gil, S., F. Vilas-Martín, A. Muñoz, J. Acosta and E. Uchupi. – 1999. Quaternary sedimentation and thermal diapirism in the Ría de Pontevedra (Galicia), Northwest Spain. *J. Coast. Res.*, 15(4): 1083-1090.

Héquette, A. and P.R. Hill. – 1995. Response of the seabed to storm-generated combined flows on a sandy arctic shoreface, Canadian Beaufort Sea. *J. Sedim. Res.*, A65 (3): 461-471.

Hovland, M. and A.G. Judd. – 1988. *Seabed pockmarks and seepages: Impact on geology, biology and marine environment*. Graham & Trotman, London: 1-293.

IGME. – 1987. *Mapa Geológico de España, E. 1:50.000 (Hojas 184, 185, 223)*. Servicio de Publicaciones Ministerio de Industria y Energía. Madrid.

King, L. H. and B. MacLean. – 1970. Pockmarks on the Scotian Shelf. *Geol. Soc. Am. Bull*., 81: 3141-3148.

Knebel, H.J. and R.C. Circé. – 1995. Seafloor environments within the Boston Harbor-Massachusetts Bay Sedimentary System: A regional synthesis. *J. Coast. Res.*, 11 (1): 230-251.

Knebel, H.J., R.R. Rendigs, J.H. List and R.P. Signell. – 1996. Seafloor environments in Cape Cod Bay, a large coastal embayment. *Mar. Geol.*, 133: 11-33.

Knebel, H.J., R.P. Signell, R.R. Rendigs, L.J. Poppe and J.H. List. – 1999. Seafloor environments in the Long Island Sound estuarine system. *Mar. Geol.*, 155: 277-318.

Kuijpers, A., F. Werner and J. Rumohr. – 1993. Sandwaves and other large-scale bedforms as indicators of non-tidal surge currents in the Skagerrak off Northern Denmark. *Mar. Geol.*, 111: 209-221.

Leckie, D. – 1988. Wave-formed, coarse-grained ripples and their relationship to hummocky cross-stratification. *J. Sedim. Petrol.*, 58(4): 607-622.

MOPU. – 1980. *Estudio de la Contaminación de la Ría de Pontevedra (SCORP I)*. Informe Técnico. Ministerio de Obras Públicas y Urbanismo. Madrid: 1-425.

Okyar, M.R. and V. Ediger. – 1997. Sea-floor sediments and bedforms around Turkey, revealed by side-scan sonar imagery. *Oceanol. Acta*, 20(5): 673-685.

Rao, P.S. – 1989. Sonograph Patterns of the Central Western Continental Shelf of India. *J. Coast. Res.*, 5(4): 725-736.

Rey, J. and T. Medialdea. – 1988. "Los sedimentos cuaternarios superficiales del margen continental español". *Spec. Publs. Inst. Esp. Oceanogr.*, 3: 224

Richtofen, F. Von. – 1886. *Führer für Forrschungsreisende*. R. Oppenheim, Berlín.

Rubio, B., L Gago, F. Vilas, M. Nombela, S. García-Gil, I. Alejo and O. Pazos. – 1996. Interpretación de tendencias históricas de contaminación por metales pesados en testigos e sedimentos de la Ría de Pontevedra. *Thalassas*, 12: 137-152.

Rubio, B., M. Nombela, F. Vilas, I. Alejo, S. García-Gil, E. García-Gil and O. Pazos. – 1995. Distribución y enriquecimiento de metales pesados de sedimentos actuales de la parte interna de la Ría de Pontevedra. *Thalassas*, 11: 35-45.

Ruíz-Mateo, A. – 1983. *Dinámica marina de la Ría de Pontevedra*. Cuad. Invest. Centro de Estudios e Investigación de Obras Públicas. Madrid.

Schmuck, E.A., P.C. Valentine and N.W. Driscoll. – 1995. Examples of trawl and dredge marks from side-scan sonar records collected from Stellwagen Bank, Georges Bank, and Block Island Sound, and their geomorphic and sedimentary significance. *Abstract Geol. Soc. Am., NE Section*, Hartford. 26(1): 80

Schwab, W.C., R. Thieler, J. S. Allen, D.S. Foster, A. Swift, J.F. Denny and W.W. Danforth. – (in press). Geologic mapping of the nearshore area offshore Fire Island, New York *Proc. Coast. Sed.*

Schwab, W.C., R.W. Rodriguez, W.W. Danforth and M.H. Gowen. – 1996. Sediment distribution on a Storm-dominated Insular Shelf. Luquillo, Puerto Rico, U.S.A. *J. Coast. Res.*, 12(1): 147-159.

Vilas, F., E. García-Gil, S. García-Gil, M.A. Nombela, I. Alejo, B. Rubio and O. Pazos. – 1996. *Cartografía de sedimentos submarinos, Ría de Pontevedra. E: 1:5000*. Ed. Xunta de Galicia, Conselleria de Pesca, Marisqueo e Acuicultura, Santiago de Compostela.

Scient. ed.: A. Palanques